

A Novel Approach to Serine Protease Inhibition: Kinetic Characterization of Inhibitors Whose Potencies and Selectivities Are Dramatically Enhanced by Zinc(II)

James W. Janc,* James M. Clark, Robert L. Warne,† Kyle C. Elrod, Bradley A. Katz, and William R. Moore

Axys Pharmaceuticals, 180 Kimball Way, South San Francisco, California 94080

Received September 21, 1999; Revised Manuscript Received February 18, 2000

ABSTRACT: Serine proteases play a role in a variety of disease states and thus are attractive targets for therapeutic intervention. We report the kinetic characterization of a class of serine protease inhibitors whose potencies and selectivities are dramatically enhanced in the presence of Zn(II). The structural basis for Zn(II)-mediated inhibition of trypsin-like proteases has recently been reported [Katz, B. A., Clark, J. M., Finer-Moore, J. S., Jenkins, T. E., Johnson, C. R., Ross, M. J., Luong, C., Moore, W. R., and Stroud, R. M. (1998) *Nature* 391, 608–612]. A case study of the kinetic behavior of human tryptase inhibitors is provided to illustrate the general phenomenon of Zn(II)-mediated inhibition. Trypsin, Zn(II), and the inhibitor form a ternary complex which exhibits classic tight-binding inhibition. The half-life for release of inhibitor from the trypsin–Zn(II)–inhibitor complex has been measured for a number of inhibitors. Consistent with tight-binding behavior, potent trypsin inhibitors are characterized by extremely slow rates of dissociation from the ternary complex with half-lives on the order of hours. A model of human serum, designed to reproduce physiological levels of Zn(II), has been employed to evaluate the performance of Zn(II)-potentiated trypsin inhibitors under physiological conditions. We demonstrate that Zn(II)-mediated inhibition can be achieved at physiological Zn(II) levels.

Serine proteases play a pivotal role in the regulation of a wide array of physiological processes, including coagulation (1), complement activation (2), and prohormone processing (3, 4). Often, such enzymes catalyze reactions which are an integral part of a cascade of biological transformations requiring exquisite regulation to maintain physiological homeostasis. By extension, serine proteases are implicated in a variety of pathological states such as inflammation (5) and tumor metastasis (6, 7) arising, in part, from misregulation or overexpression of certain proteases. Thus, the proteases implicated in these disease states may represent attractive targets for therapeutic intervention.

As part of our effort to develop therapeutics targeting serine proteases, we have discovered a novel means for inhibiting proteases in which Zn(II) potentiates the inhibition of active site-directed, small molecule inhibitors (8). With trypsin, Katz and co-workers have shown that Zn(II) plays a direct role in mediating a high-affinity binding mode in which Zn(II) is simultaneously coordinated to O- γ of Ser195 and N- ϵ 2 of His57 (trypsin numbering system) as well as to two chelating elements supplied by the inhibitor (see Figure 1). This “bridging” of inhibitor to the active site mediated by Zn(II) routinely affords 1000-fold binding enhancement (8), and in some cases, the enhancement has been as high as 100000-fold (vide infra). This mode of inhibition relies on the spatial presentation of the catalytic triad which, from structural studies, is known to be strictly conserved among

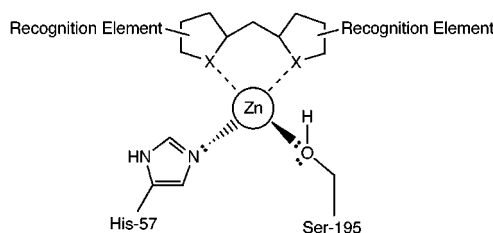


FIGURE 1: General paradigm for Zn(II)-mediated inhibition of serine proteases. Two ligands to Zn(II) are supplied by the protease, and two ligands (X, a chelating heteroatom such as N, O, or S) are supplied by the inhibitor. The recognition elements can be optimized for the serine protease target of interest.

trypsin-like serine proteases. This being the case, the authors were able to demonstrate potent Zn(II)-mediated inhibition with several trypsin-like enzymes, including thrombin and factor Xa (8).

In this study, we have applied Zn(II)-mediated inhibition to human tryptase to illustrate the general utility of this novel approach to serine protease inhibition. Tryptase (EC 3.4.21.59) is a tetrameric, trypsin-like serine protease found at high concentrations in mast cell secretory granules (9, 10). Tryptase has been shown to heighten the sensitivity and magnitude of the response to histamine-induced bronchoconstriction without affecting smooth muscle tone (11). Thus, specific inhibitors of tryptase may attenuate the bronchial hyper-responsiveness to histamine seen in asthmatics. Indeed, APC-366, an active site-directed tryptase inhibitor, has been shown to block allergen-induced airway hyper-responsiveness and inflammatory responses in allergic sheep (12). The aim of the study presented here was to provide kinetic and biochemical characterization of Zn(II)-mediated inhibition of serine proteases. Human tryptase, a representative serine

* To whom correspondence should be addressed. E-mail: james_janc@axyspharm.com. Phone: (650) 829-1136. Fax: (650) 829-1350.

† Current address: Chiron Corp., 4560 Horton St., Emeryville, CA 94608.

protease of therapeutic interest, has been featured to highlight the general utility of Zn(II)-mediated inhibition.

MATERIALS AND METHODS

Tryptase used in this study was purified from an HMC-1¹ cell line, provided by J. Butterfield of the Mayo Clinic (Rochester, MN), according to established protocols (13). All other enzymes used in this study were of human origin and were obtained from commercial sources. The substrate used to measure tryptase, trypsin, and thrombin catalytic activity, tosyl-Gly-Pro-Lys-*p*-nitroanilide, and human serum albumin were purchased from Sigma Chemical Co. (St. Louis, MO). The inhibitors APD-9–13 were synthesized by Axys Pharmaceutical Corp. The synthesis of representative members of this collection has been described previously (14). ZnCl₂ (>99.999% pure) was obtained from Aldrich (Milwaukee, WI). All other chemicals were of the highest available quality.

K_i' Determinations. Tryptase inhibition studies were performed in 50 mM Tris (pH 8.2), 100 mM NaCl, 0.05% polyoxyethylenesorbitan monolaurate (Tween 20), 50 μg/mL heparin, and 10% DMSO. Tryptase (1.0 nM active sites) was incubated with inhibitor, present at varying concentrations, for 1 h at room temperature (21–24 °C) in 96-well microtiter plates. Typically, the evaluation of a given inhibitor's potency was determined under two distinct sets of experimental conditions. In one set of assay conditions, ZnCl₂ was supplied at 150 μM. In parallel experiments, the inhibitor was evaluated without Zn(II) supplementation and with 1.0 mM EDTA included in the standard assay. After preincubation, reactions were initiated with the addition of the chromogenic substrate, tosyl-Gly-Pro-Lys-*p*-nitroanilide (final concentration was 0.5 mM). The hydrolysis of this substrate yields *p*-nitroaniline which was monitored spectrophotometrically at 405 nm ($\epsilon = 14\,400\text{ M}^{-1}\text{ cm}^{-1}$) (15). The velocity of the tryptase-catalyzed reaction was obtained from the linear portion of the progress curves using a UV/MAX kinetic microplate reader (Molecular Devices, Sunnyvale, CA) interfaced with a Macintosh Quadra 840 computer. Apparent inhibition constants, *K_i'*, were calculated from the velocity data generated at the various inhibitor concentrations using the software package Batch *K_i* (obtained from P. Kuzmic, Biokin Ltd., Madison, WI) (16). Batch *K_i* provides a parametric method for the determination of inhibitor potency using a transformation (17) of the tight binding inhibition model described by Morrison (18), and further refines the *K_i'* values by nonlinear least-squares regression (19).

Measurement of Metal Binding Affinity of Inhibitors. Equilibrium binding constants for the class of bis-benzimidazole methane inhibitors were determined by titration of an aqueous solution of inhibitor with a solution of divalent cation. A 1 mL solution of inhibitor (20 μM) in dilute Tris buffer (5.0 mM, pH 8.0) was prepared in a cuvette with a path length of 1 cm. Constant ionic strength was maintained with LiClO₄ ($\mu = 0.1$). The optical spectrum of the

compound was recorded from 200 to 400 nm using a Shimadzu-160 UV–vis spectrophotometer equipped with a thermostated cell compartment. Constant temperature was maintained at 25 °C. An aliquot of divalent cation was added to the cuvette, and the change in the optical spectrum of the compound was recorded. Further additions of divalent cation were made, and each resulting spectrum was recorded. Graphical analysis of the change in absorbance at a fixed wavelength was used to calculate the dissociation constant for Zn(II) (or other cation). The actual wavelength used for determination of the *K_d* is unique to the inhibitor–cation pair. The metal ion concentration divided by the change in absorbance ($\Delta A = \text{measured absorbance} - \text{absorbance of the unbound ligand}$) was plotted versus the metal ion concentration. This method of data analysis yields a straight line from which the value of *K_d* can be extracted from the ratio of the *y*-intercept to the slope as defined by the Scott equation (eqs 1 and 2) (20).

$$[\text{M(II)}]/\Delta A = [\text{M(II)}]/([\text{ligand}]\Delta\epsilon) + 1/([\text{ligand}]\Delta\epsilon) \quad (1)$$

$$K_a = 1/K_d = \text{slope}/y\text{-intercept} \quad (2)$$

Double-Inhibition Studies. Kinetic data were fitted to the appropriate equation with the FORTRAN programs of Cleland to obtain the desired kinetic parameters (21). Competitive inhibition data were fitted to eq 3 where *V* is the maximal velocity, *A* is the concentration of the substrate, *K* is the Michaelis constant (*K_m*), *I* is the concentration of the variable inhibitor, and *K_{is}* is the dissociation constant for the E–I complex. Data from double-inhibition experiments were fitted to eq 4 where *I* and *J* are concentrations of the variable inhibitors and *K_i* and *K_j* are the dissociation constants for the E–I and E–J complexes, respectively. The factor α is the synergy factor as defined by Yonetani and Theorell (22).

$$v = VA/[K(1 + I/K_{is}) + A] \quad (3)$$

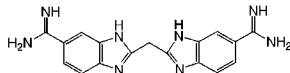
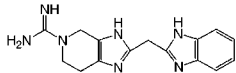
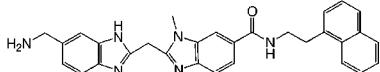
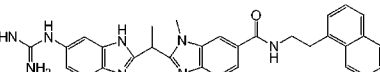
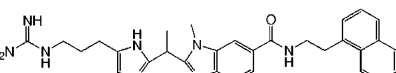
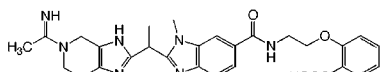
$$v = V/(1 + I/K_i + J/K_j + IJ/\alpha K_i K_j) \quad (4)$$

Tryptase velocity measurements were performed under the assay conditions described above. Kinetic measurements were made with a Shimadzu-160 UV–vis spectrophotometer equipped with a thermostated cell compartment. Reactions were initiated with the addition of enzyme. Initial velocity measurements were performed in a total volume of 1 mL in cuvettes with a path length of 1 cm. Constant temperature was maintained at 25 °C. Double-inhibition experiments were performed by varying the concentration of inhibitor from 0 to 2.4 μM at several levels of Zn(II) ranging from 5 to 100 μM. The concentration of substrate, tosyl-Gly-Pro-Lys-*p*-nitroanilide, was fixed at 0.5 mM.

Progress Curve Analysis. The analysis of slow, tight-binding inhibitors was performed according to the method of Walsh and Morrison (23). Progress curves were measured under the standard conditions described above. A Cary BioSpec 1 apparatus, equipped with a thermostated cell compartment, was used to measure the progress curves. Constant temperature was maintained at 25 °C. Product–time data were fitted to eq 5 in which *P* is the product concentration at time *t*, *v_o* is the initial rate of substrate

¹ Abbreviations: BABIM, bis(5-amidino-2-benzimidazolyl)methane; DMSO, dimethyl sulfoxide; EDTA, ethylenediaminetetraacetic acid; HEPES, *N*-(2-hydroxyethyl)piperazine-*N'*-2-ethanesulfonic acid; HMC, human mast cell; HSA, human serum albumin; Tris, *N,N,N*-tris(hydroxymethyl)aminomethane.

Table 1: Potency and Selectivity Parameters for Selected Zn(II)-Mediated Tryptase Inhibitors

APD #	Compound	Tryptase		Zn(II) Enhancement Factor	Trypsin	Thrombin
		K_i' (nM) [+Zn(II)]	K_i' (nM) (+EDTA)		K_i' (nM) [+Zn(II)]	K_i' (nM) [+Zn(II)]
1		3.7	1,500	400	10	20
9		500	280,000	600	5,000	60
10		0.068	6,600	97,000	670	> 1,000,000
11		6.2	3,700	600	30,000	92,000
12		2.7	8,800	3,300	800,000	8,300
13		6.9	390,000	57,000	1,700	37,000

hydrolysis, v_s is the final steady-state rate, and k_{obs} is the apparent first-order rate constant for the transformation of the E–I complex to the E–I* complex.

$$P = v_s t - (v_s - v_o)(1 - e^{-k_{obs}t})/k_{obs} \quad (5)$$

Off-Rate Determination. The off-rate of dissociation of the inhibitor from the ternary complex was determined by performing the tryptase–Zn(II)–inhibitor complex during a 1 h incubation phase. Following this incubation phase, reactions were quenched with the addition of EDTA (1 mM). The recovery of tryptase activity following release of the inhibitor and sequestration of Zn(II) by EDTA was monitored as a function of time using the standard tryptase activity assay described above. Typical reaction mixtures contained tryptase (1.0 nM) in 50 mM Tris (pH 8.2), 100 mM NaCl, 0.05% Tween 20, 50 μ g/mL heparin, and 5% DMSO. Zinc(II) was present at a concentration of 25 μ M. Inhibitors were supplied at 20–200-fold stoichiometric excess over tryptase active sites (20–200 nM). Control experiments were performed in which Zn(II) or the inhibitor was excluded from the incubation phase.

Human Serum Albumin Studies. The standard assay of tryptase and assessment of inhibitor potency was performed as previously described with the following modifications. Human serum albumin (HSA) was included in the reaction mixture at a concentration of 450 μ M (30 mg/mL). Antifoam-B, a nonionic emulsifier (from Sigma Chemical Co.), was included in the assay at 0.002% to avoid excessive foaming at high concentrations of HSA. The concentration of Zn(II) supplied with 450 μ M HSA was determined by atomic absorption spectroscopy to be 18 μ M (determined by Galbraith Laboratories, Inc., Knoxville, TN). Reactions were conducted at pH 7.4, and the mixtures were supplemented

with exogenous ZnCl₂ to bring the final Zn(II) concentration in the assays to 28 or 123 μ M. These levels of ZnCl₂ yield free Zn(II) concentrations of 2.2 and 12.5 nM, respectively, given the fact that the K_d for Zn(II) for the high-affinity binding site of human serum albumin is 30 nM (24). The level of free Zn(II) in the assay was chosen to approximate the value reported in the literature for human plasma, estimated to be 1 nM (25). The inhibitory potency, K_i' , of APD-12 in this HSA/Zn(II) buffering system was measured as a function of time.

RESULTS

Zn(II)-Mediated Inhibition. We have characterized the inhibition of human tryptase by a class of compounds whose potency is dramatically increased in the presence of Zn(II). The apparent inhibition constants (K_i') for a representative collection of inhibitors were determined under one of two sets of experimental conditions. Inhibitors were evaluated in the presence 150 μ M Zn(II) or in the presence of 1 mM EDTA. With APD-1 and APD-9, two simple, unoptimized tryptase inhibitors, Zn(II) enhances the potency of these inhibitors several 100-fold against tryptase, trypsin, and thrombin (Table 1, EDTA data not shown for trypsin and thrombin). In some instances, the Zn(II)-dependent enhancement of K_i' approaches 10⁵-fold over the parallel K_i' determination in the presence of EDTA (APD-10, Table 1). High selectivity for tryptase over other closely related lysine/arginine-selective endoproteases starting from the nonspecific protease inhibitor bis(5-amidino-2-benzimidazolyl)methane (BABIM, APD-1) originally reported by Tidwell and co-workers (26) was also achieved. For instance, APD-10, a 68 pM tryptase inhibitor in the presence of Zn(II), has been optimized through iterative medicinal chemistry to be 10000-fold selective for tryptase over the closely related enzymes

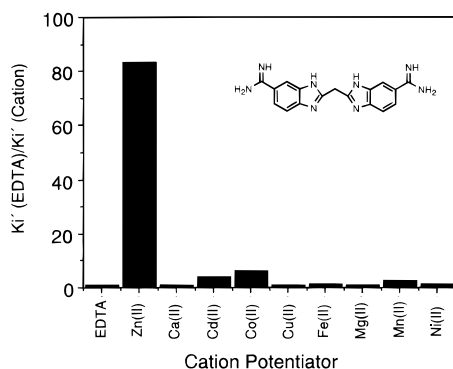


FIGURE 2: Potentiation of trypsin inhibition by bis(5-amidino-2-benzimidazolyl)methane (BABIM, APD-1) in the presence of selected divalent cations. The K'_i for the inhibitor in the presence of the specified cation ($100 \mu\text{M}$) was determined using the trypsin assay described in Materials and Methods. Data are expressed as a ratio of the K'_i in EDTA (no metal condition) divided by the K'_i obtained in the presence of the specified cation ($100 \mu\text{M}$).

trypsin and thrombin. The free energy gain associated with the favorable interaction that Zn(II) imparts in bridging the trypsin–inhibitor complex is calculated to be on the order of 4–7 kcal/mol (at 25°C).

We tested the possibility that cations other than Zn(II) might potentiate the inhibitory properties of bis-benzimidazole methane inhibitors. Cations were supplied in the standard assay at a concentration of $100 \mu\text{M}$. The divalent cations Ca(II), Cu(II), Mg(II), and Ni(II) do not elicit significant enhancement of inhibitor potency (see Figure 2). Slight potentiation, generally less than 10-fold, was observed with Cd(II), Co(II), and Mn(II). The crystal structure of an analogue of APD-1 bound to trypsin in the presence of Co(II) reveals a binding mode virtually identical to that seen in the APD-1–Zn(II) complex (8), suggesting that Co(II) is indeed capable of potentiating serine protease inhibition *in vitro*. Cd(II), a nonphysiological metal, and Co(II) are unlikely to be available in a biologically exchangeable form. The slight potentiation by Mn(II), although a physiologically available cation, does not appear to offer sufficient enhancement of binding to be of therapeutic interest. Thus, of the cations that might be exploited for therapeutic application of metal-mediated inhibition, only Zn(II) appears to have the requisite properties. The physical basis for this observation resides in the unique capability of Zn(II) to coordinate a variety of ligand types, arranged in any of several possible geometries, as a consequence of its completely filled d electron shell (27).

Measurement of Metal Binding Affinity of Inhibitors. A variety of methods are available for the determination of metal binding constants. We chose to utilize optical spectroscopy to investigate the metal binding properties of bis-benzimidazole methane inhibitors. Equilibrium binding constants were determined by titration of an aqueous solution of inhibitor with a solution of divalent cation. The UV–vis spectrum of APD-10 was recorded as a function of Zn(II) concentration. The metal–ligand interaction was assumed to follow a two-state equilibrium. Consistent with this assumption, a well-defined isosbestic point was observed in the titration of APD-10 with Zn(II). A plot of the negative change in absorbance ($-\Delta A$) at 222.2 nm [the wavelength where the maximum change in APD-10 absorbance upon complexation with Zn(II) was observed] versus Zn(II)

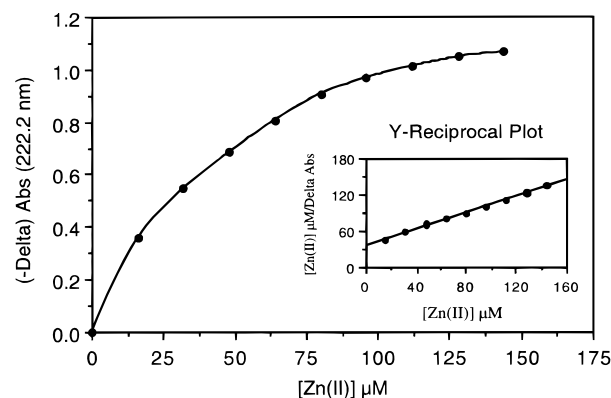


FIGURE 3: Measurement of the binding constant of APD-10 for binding to Zn(II). The change in the optical spectrum of APD-10 at 222.2 nm was plotted as a function of the total Zn(II) concentration. The binding isotherm, describing a rectangular hyperbola, was replotted as the y-reciprocal according to the method of Scott (19) (inset of Figure 2). The K_d obtained for the Zn(II)–APD-10 complex is $51 \pm 2 \mu\text{M}$ (25°C and $\mu = 0.1$).

Table 2: Summary of the Dissociation Constants for Selected Cations with APD-10^a

divalent cation	K_d (μM)
Zn(II)	51 ± 2
Cu(II)	12 ± 2
Ni(II)	270 ± 10
Co(II)	370 ± 30

^a Values were obtained at 25°C . Constant ionic strength was maintained with LiClO_4 ($\mu = 0.1$).

concentration yielded a rectangular hyperbola (see Figure 3). Linerization of the data allows for direct extraction of the dissociation constant (K_d) for the APD-10–Zn(II) complex from the ratio of the y-intercept to the slope (see the inset of Figure 3). The K_d value obtained for the APD-10–Zn(II) complex was $51 \pm 2 \mu\text{M}$. This value is consistent with literature values for related scaffolds such as 2-(2-pyridyl)imidazole which has a K_d for Zn(II) of $41 \mu\text{M}$ (28). The affinity of APD-10 for a collection of first-row transition metals was measured and compared with the affinity of APD-10 for Zn(II) (see Table 2). Of the cations tested, APD-10 has the highest affinity for Cu(II) followed, in order, by Zn(II), Ni(II), and Co(II). This general trend is consistent with the binding affinity for first-row transition metal–ion complexes predicted by Irving and Williams (29).

Double-Inhibition Studies. The combined effect of two linear competitive inhibitors on a single enzyme target can yield important insight into the nature of the inhibitor binding sites and the extent to which two inhibitors interact when bound to the enzyme. Yonetani and Theorell (22) developed a graphical method for extracting quantitative information from such a system. The general form of the equation (eq 4) used in this analysis defines a synergy factor α . The coefficient, α , provides a measure of the interaction of the two inhibitors in the ternary complex. An infinite value for α implies that the binding of the two inhibitors is mutually exclusive, whereas finite values for α indicate that the two inhibitors can occupy the active site simultaneously. A finite α value of > 1 indicates an antisynnergistic relationship exists between the two inhibitors in the E–I–J complex, implying a degree of interference between the two inhibitors when bound. An α value of 1 indicates no interaction between the

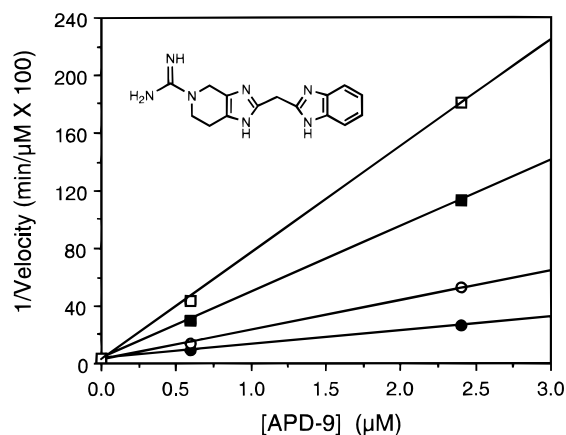


FIGURE 4: Double-inhibition studies for inhibition of trypsin by APD-9 and Zn(II). Trypsin inhibition studies were performed in 50 mM Tris (pH 8.2), 100 mM NaCl, 0.05% polyoxyethylene-sorbitan monolaurate (Tween 20), 50 $\mu\text{g}/\text{mL}$ heparin, and 10% DMSO. The APD-9 concentration was varied from 0 to 2.4 μM at four levels of Zn(II). Zinc was supplied at a concentration of 5 (\bullet), 15 (\circ), 40 (\blacksquare), and 100 μM (\square).

two inhibitors at the active site when they are simultaneously bound. Finally, an α value of <1 indicates that a synergistic relationship exists in binding of the two inhibitors to the E–I–J ternary complex. The parameters αK_i and αK_j are apparent dissociation constants for dissociation from the E–I–J complex of inhibitors I and J, respectively. Double-inhibition data are typically plotted as reciprocal velocity versus concentration of I at different fixed levels of J (30, 31). Two patterns are possible with this type of presentation. When α is finite, an intersecting pattern is expected. When α is infinite, a family of parallel lines will be generated. When analyzed independently, both APD-9 and Zn(II) are linear competitive inhibitors of trypsin with apparent K_i values of 280 μM (under typical metal-free assay conditions) and 2 mM, respectively (data not shown). We examined the inhibition of trypsin at varying levels of Zn(II) and APD-9. In the presence of varied Zn(II) levels, a family of intersecting lines was obtained (see Figure 4). The value obtained for α from fitting the data to eq 4 was 0.011. This small value is diagnostic of a highly synergistic interaction in the trypsin–Zn(II)–APD-9 ternary complex. The apparent dissociation constant for APD-9 for dissociation from the ternary complex, αK_i , is 530 nM, corresponding to a 500-fold binding enhancement relative to APD-9 interacting with free enzyme ($K_i = 280 \mu\text{M}$).

Progress Curve Analysis. An examination of the kinetics of trypsin inhibition by APD-9 in the presence of Zn(II) revealed nonlinear progress curves (see Figure 5). This observation is consistent with a slow, tight-binding mechanism of trypsin inhibition (32, 33). The progress curves were fit to eq 5, which describes the expected behavior of a slow, tight-binding inhibitor. This analysis yields reasonable estimates for k_{obs} , the apparent first-order rate constant at each level of APD-9 in the presence of a fixed concentration of Zn(II). Subsequent replot analysis of k_{obs} versus APD-9 concentration revealed a hyperbolic dependence of k_{obs} on inhibitor concentration (see the inset of Figure 5). This hyperbolic dependence of k_{obs} on inhibitor concentration is consistent with the prior formation of an initial complex (capable of saturation by APD-9) followed by the slow conversion to a tightly bound complex. The K_{app} for APD-9

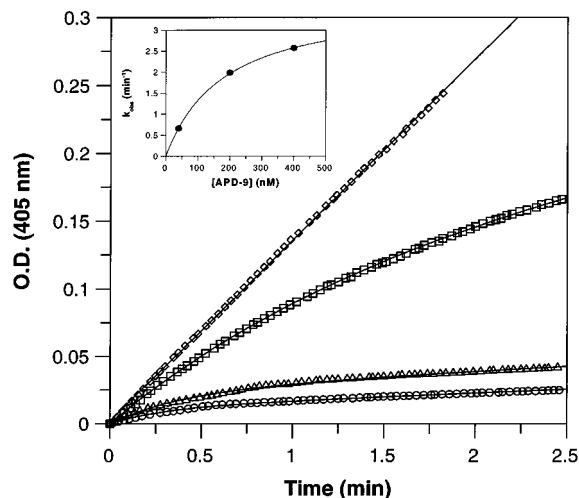
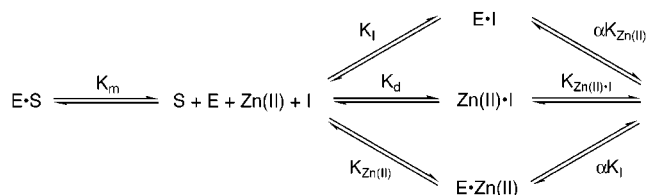
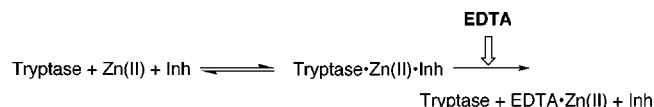


FIGURE 5: Progress curves illustrating the slow, tight binding of APD-9 to trypsin in the presence of Zn(II). The hydrolysis of tosyl-Gly-Pro-Lys-*p*-nitroanilide (present at 1.0 mM) was monitored at 405 nm under conditions described in Materials and Methods. Reactions were initiated with the addition of trypsin (10 nM). The concentration of Zn(II) was fixed at 40 μM . APD-9 was present in varying amounts: 0 (\diamond), 40 (\square), 200 (\triangle), and 400 nM (\circ). The symbols represent the experimental data, while the curve represents the best fit to eq 5. The k_{obs} value obtained at each concentration of APD-9 from the fit to eq 5 was replotted vs the concentration of inhibitor (inset of Figure 5). The data were fitted to a rectangular hyperbola (the curve represents the fit to the experimental data) which yields a K_{app} value of 180 nM for APD-9.

obtained from the replot analysis is 180 nM. This value is 4600-fold lower than the K_i for APD-9 measured in the absence of Zn(II) (840 μM , corrected for 1.0 mM substrate). The enhanced potency of APD-9, as determined from the progress curve analysis, suggests that Zn(II) is potentiating the binding of APD-9 in the loosely bound complex. Thus, Zn(II) must be present in the initial ternary complex. The initial, loosely bound complex then slowly converts to the tightly bound ternary complex, trypsin–Zn(II)–APD-9*. There are likely to be three competing pathways for the generation of the initial trypsin–Zn(II)–APD-9 ternary complex (see Scheme 1). The preferred pathway for the formation of the initial ternary complex cannot be deciphered from steady-state kinetics; however, it is likely that all three pathways contribute (to varying extents) to the generation of the first ternary complex. It is also likely that different enzyme systems will favor one pathway over the others and, thus, the rapid equilibrium phase will vary from system to system. For example, in cases where the intrinsic affinity of the inhibitor for Zn(II) is very high, the path in which the Zn(II)–inhibitor binary species directly binds to the enzyme would be favored.

Off-Rate Determination. Investigation of the tight-binding behavior displayed by the compounds described in this report was studied with the specific aim of measuring the off-rate constant that governs the dissociation of the Zn(II)–inhibitor species from the ternary complex (Scheme 1). Trypsin was incubated with Zn(II) and inhibitor under conditions which favor the formation of the trypsin–Zn(II)–inhibitor complex. Following this incubation phase required for the formation of the ternary complex, EDTA was added to the reaction mixtures. As inhibitor and Zn(II) dissociate from the enzyme, Zn(II) is sequestered by excess EDTA and the catalytic activity of trypsin is restored (see Scheme 2). If

Scheme 1: Kinetic Scheme Illustrating Three Potential Pathways for the Generation of the Enzyme–Zn(II)–Inhibitor Ternary Complex

Scheme 2: Strategy for Measuring the Dissociation Rate of Inhibitor from the Trypsin–Zn(II)–APD-13 Complex^a

^a The time-dependent restoration of trypsin activity was measured following sequestration of Zn(II) with EDTA.

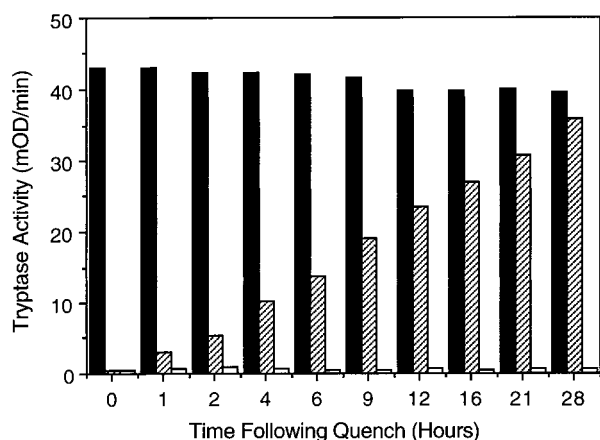


FIGURE 6: Recovery of trypsin activity following EDTA quenching of the trypsin–Zn(II)–APD-13 complex. The solid bars correspond to trypsin preincubated with APD-13 in the absence of Zn(II). The hatched bars correspond to the reaction in which trypsin, Zn(II), and APD-13 were incubated for 1 h and then quenched with EDTA. The open bars correspond to enzyme exposed to Zn(II) and APD-13 but was not quenched with EDTA. The x-axis corresponds to time following quenching and does not include the incubation period.

the inhibitor bound to trypsin in a rapid equilibrium fashion, one would expect to observe the immediate restoration of trypsin activity upon EDTA quenching. If, however, there is slow release of the inhibitor from the ternary complex, one would expect to observe a measurable dissociation rate (34). Indeed, the latter scenario was observed in which we measured a substantial time dependence for the restoration of trypsin activity following EDTA quenching. Representative data for the recovery of trypsin activity following EDTA quenching of the trypsin–Zn(II)–APD-13 complex are presented in Figure 6. In control experiments, trypsin that was pretreated with EDTA during the incubation phase was not subject to inhibition under the condition used for the assay (solid bars). Trypsin that was allowed to form the ternary complex but was not quenched with EDTA remained inhibited throughout the entire course of the experiment (open bars). Trypsin that was preincubated with Zn(II) and APD-13 for 1 h was completely inhibited. Following EDTA addition to this sample, aliquots were assayed for trypsin activity. A time-dependent return in trypsin activity was observed (hatched bars). The log of the % trypsin inhibited was plotted as a function of time for the enzyme inhibited

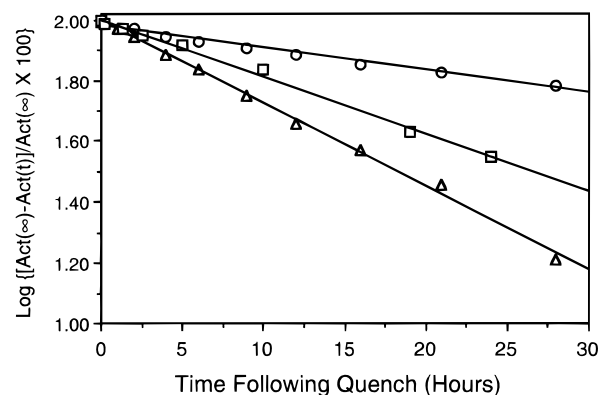


FIGURE 7: Extraction of the first-order rate constants for the dissociation of selected inhibitors from their respective ternary complexes. The log of the percent of total trypsin activity (obtained from Figure 6 for APD-13) vs time is plotted to determine k_{off} for APD-13 (Δ), APD-12 (□), and APD-10 (○).

with APD-10, APD-12, and APD-13 (see Figure 7). From the slope of each line, one is able to extract the off-rate constant (k_{off} , Scheme 1) for each inhibitor. In all cases, the rate at which trypsin activity was recovered corresponded to a first-order process. The off-rate data together with the half-lives for these three trypsin–Zn(II)–I complexes are summarized in Table 3. The off-rate data correlate with the inhibitor potency in the presence of Zn(II). For example, APD-10, the most potent of the trypsin inhibitors examined in this study, possessed the slowest rate of dissociation from the ternary complex ($t_{1/2} = 32$ h).

In related control experiments, we varied the concentration of EDTA used to quench the ternary complex. We found that the EDTA concentration used to reverse the inhibition did not affect the rate at which trypsin activity was restored (data not shown). This is consistent with the release of inhibitor being a strictly first-order process dictated by k_{off} and ultimately the thermodynamic stability of the ternary complex. An additional control was performed in which we attempted to observe the exchange of radiolabeled APD-11 into the ternary complex. We found that the rate at which [³H]APD-11 was incorporated into the trypsin–Zn(II)–APD-11 complex (prepared with radioinactive APD-11) was identical to the rate at which trypsin activity was restored following EDTA addition. Again, this result is consistent with the kinetic path outlined in Scheme 1 in which the release of inhibitor from the ternary complex is dominated by k_{off} . Further, these experiments eliminate the possibility that Zn(II) and the inhibitor are able to dissociate faster than the off-rate measured upon EDTA quenching. This is consistent with a rapid-equilibrium establishment of the trypsin–Zn(II)–inhibitor ternary complex followed by the slow first-order transition to the trypsin–Zn(II)–inhibitor*

Table 3: Summary of the Dissociation Rate Constants for Selected Tryptase Inhibitors

APD #	Compound	K_i' (nM) [+Zn(II)]	k_{off} (hr ⁻¹)	$t_{1/2}$ (hrs)
10		0.068	0.022	32
12		2.7	0.043	16
13		6.9	0.065	11

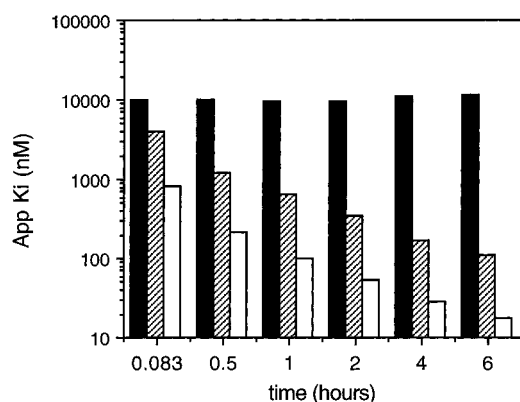


FIGURE 8: Measurement of the extent of tryptase inhibition by APD-12 in a model of human serum in which human serum albumin has been employed as a Zn(II) buffering agent. The standard assay of tryptase and assessment of inhibitor potency was performed as described in Materials and Methods. Human serum albumin (HSA) was included in the assay buffer at a concentration of 450 μ M (30 mg/mL). Reactions were conducted at pH 7.4, and the mixtures were supplemented with exogenous $ZnCl_2$ such that the free concentration of Zn(II) was 2.2 (hatched bars) and 12.5 nM (open bars). The solid bars correspond to the inhibition of tryptase in HSA containing buffer supplemented with 1 mM EDTA. The inhibitory potency, K_i' , of APD-12 in this HSA/Zn(II) buffering system was measured as a function of time.

complex as supported by the progress curve analysis (vide supra).

Human Serum Albumin Studies. An assay system was developed to assess the potency of tryptase inhibitors in a medium with a defined Zn(II) concentration which reflects the level of Zn(II) found in human serum. It is known that the bulk of exchangeable Zn(II) in serum is bound to serum albumin (35). The K_d for Zn(II) for the high-affinity metal binding site of albumin is 30 nM (24, 36). The assay we developed supplies human serum albumin and Zn(II) at levels which reflect those found in vivo (35, 37). The evaluation of tryptase inhibition by APD-12 in this system revealed that there was sufficient Zn(II) to potentiate the inhibition of tryptase (Figure 8). With extended time, the potency of APD-12 inhibition increased, suggesting the available Zn(II), buffered by HSA, was accessible and was sufficient to drive the formation of the ternary complex. Control experiments

in which EDTA was supplied in place of Zn(II) revealed only weak ($K_i' = 10 \mu$ M) inhibition of tryptase by APD-12 (solid bars, Figure 8). Further, there was no time-dependent increase in inhibitor potency in the EDTA control experiments. This experiment suggests that, given sufficient time to establish equilibrium and sufficient potency of the ternary complex, Zn(II)-mediated inhibition can be achieved at the low, free levels of Zn(II) which exist in plasma.

DISCUSSION

Zn(II) plays an important role in a variety of biological processes (38). In many instances, Zn(II) plays a structural role in the maintenance of the three-dimensional structure of a protein as is the case with zinc-finger proteins (39, 40). In other cases, Zn(II) directly participates in the chemistry catalyzed by certain enzymes, a notable example being the Zn(II)-metallo protease family of enzymes (41). Zn(II) has been shown to mediate interactions between macromolecules such as human growth hormone and the prolactin receptor (42) and to accelerate the activation of factor XII by plasma kallikrein as part of the intrinsic pathway of the coagulation cascade (43). The activity of recombinant trypsin, mutagenized to contain a metal binding site, can be modulated by Zn(II) (44). We now describe yet another role in which Zn(II) potentiates the inhibitory interaction between low-molecular weight chelating inhibitors and a serine protease.

Structural studies with trypsin have revealed that Zn(II) plays a direct role in bridging the inhibitor to the active site the enzyme (8). We have extended this finding by applying this mode of inhibition to human tryptase. A model of the active site of tryptase in which His44 and Ser194 of the catalytic triad are chelated to Zn(II) along with two benzimidazole nitrogens from APD-10 is provided in Figure 9. The benzylamine recognition element of APD-10 was incorporated into the molecule to make a favorable interaction with Asp189 in the S1 subsite of tryptase. The prime-side-directed naphthyl amide recognition element was discovered through iterative medicinal chemistry and in part provides the selectivity for tryptase over thrombin and trypsin. Kinetic studies have revealed that the Zn(II)-mediated binding mode is highly synergistic and imparts from 4 to 7 kcal/mol of stabilization, resulting in as much

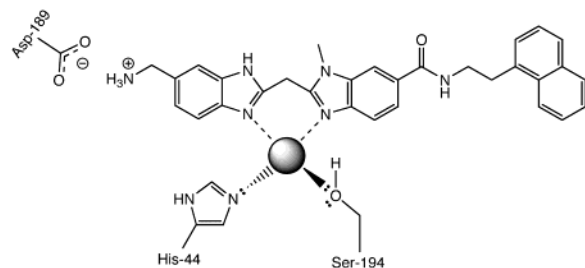
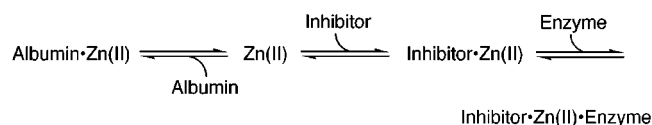


FIGURE 9: Zn(II)-mediated inhibition of trypsin by APD-10.

Scheme 3: Pathway for the Establishment of an Inhibited Target Protease in Human Serum



as a 10^5 -fold binding enhancement. An analysis of related divalent cations indicated that the binding mode is quite specific for Zn(II). Other metals such as Co(II) and Mn(II) will support the formation of the ternary complex, albeit with much less avidity.

Zn(II)-potentiated inhibition represents a unique approach to the design of therapeutics directed at serine protease targets. However, at least two major factors must be addressed in the application of this technology to drug design. First, Zn(II)-dependent inhibitors must function effectively in environments where most of the Zn(II) is sequestered by proteins or other endogenous chelators, a requirement unique to this class of compounds. Second, the inhibitors must be selective for their enzyme target, a requirement shared by all protease inhibitors intended for therapeutic use. Estimates of free Zn(II) concentrations in plasma range from 200 pM in equine plasma (45) to 1 nM in human plasma (25). However, the total Zn(II) concentration in plasma is approximately 15 μ M (46), of which two-thirds is loosely bound by albumin and is considered exchangeable (47, 48). We modeled the *in vivo* situation by including albumin in the assay to provide buffered Zn(II) at physiological levels. In this assay, APD-12 shows a significant Zn(II)-dependent enhancement, indicating that inhibition of the target protease can be achieved at physiological levels of exchangeable Zn(II). Further, we have shown through the refinement of the chelation scaffold that subtle differences among the active sites of closely related enzymes can be exploited to yield highly selective inhibitors (Table 1). Thus, two of the major issues in applying this concept to drug development are amenable to resolution through structural modifications of the core Zn(II) chelation scaffold.

The availability of Zn(II) and the thermodynamic stability of the enzyme–Zn(II)–inhibitor ternary complex are the dominant factors affecting the utility of Zn(II)-mediated inhibition. A simple model system incorporating these factors in describing the equilibrium involved in forming the ternary complex for an inhibitor in plasma can be defined as in Scheme 3. Using this model, we have attempted to predict the effectiveness of Zn(II)-mediated inhibitors in plasma. This analysis assumes that the system is closed, at equilibrium, and that the starting concentrations of albumin, Zn(II), inhibitor, and enzyme and the K_d for the Zn(II)–albumin complex are constants. We also assume that Zn(II) is buffered

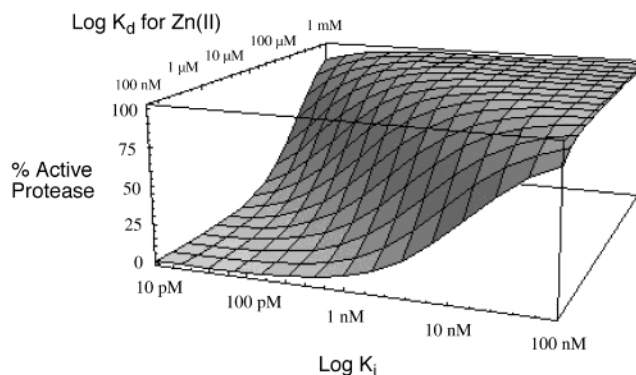


FIGURE 10: Three-dimensional representation of the inhibition of a protease by a Zn(II)-mediated inhibitor. Discrete solutions were determined assuming 450 μ M albumin, 10 μ M Zn(II), 1 nM enzyme, 2 μ M inhibitor, and a K_d for the albumin–Zn(II) complex equal to 30 nM. The graph was generated using Mathematica (Wolfram Research, Inc.). The K_d for the inhibitor–Zn(II) complex was allowed to vary from 1 to 100 nM (y-axis), and the K_i for the enzyme–Zn(II)–inhibitor complex was allowed to vary from 100 nM to 10 pM (x-axis). The closed system in Scheme 3 was solved for the fraction of active protease (z-axis).

exclusively by albumin, ignoring the relatively minor contributions of other plasma Zn(II) ligands such as histidine and cysteine (49). Thus, the concentration of the Zn(II)–inhibitor species is a function of the inhibitor's affinity for Zn(II) and is defined by the concentrations of Zn(II), albumin, and inhibitor. The fraction of enzyme that is inhibited is assumed to be a function of the concentration of the Zn(II)–inhibitor complex and the affinity of this species for the enzyme. Subject to these constraints, a series of equations representing the coupled equilibria in Scheme 3 can be generated. Solving these equations simultaneously yields the percent active protease as a function of the affinity of the inhibitor for Zn(II) and the potency of the Zn(II)–inhibitor complex for the target enzyme, represented graphically in Figure 10. Although more complex equilibria can be envisioned for the assembly of the ternary complex, this simplified theoretical analysis accurately predicts the *in vitro* activity of inhibitors tested in our plasma model. The data furthermore suggest that an important design criterion for efficacious inhibitors is sufficient intrinsic metal binding affinity. This analysis, together with our experimental data, suggests that effective inhibition can be achieved in plasma *in vivo*, given sufficient intrinsic metal binding affinity and intrinsic potency of the Zn(II)–inhibitor complex.

A compound intended for therapeutic use clearly must incorporate both high selectivity and the ability to compete for Zn(II) in the appropriate tissue or plasma compartment. Recent progress in inhibitor design has proven that such a goal is achievable, and that Zn(II)-potentiated inhibition can be extended to enzymes other than serine proteases that have appropriate chelating functionalities at their active sites. Clearly, all that is required for the successful application of this approach is that the target active site possess the appropriately disposed chelation functionality. To date, only Zn(II) appears to have both the requisite chemical properties and biological availability to support therapeutic applications of the phenomenon of metal-mediated inhibition. The ability of Zn(II) to potentiate the activity of small molecule serine protease inhibitors via the formation of a ternary enzyme–

Zn(II)–inhibitor complex is yet another example of the remarkable versatility of this metal ion in biological systems.

ACKNOWLEDGMENT

We thank Dr. T. Jenkins, Dr. J. Spencer, M. Linsell, P. Fatheree, and T. Church for the synthesis of the inhibitors used in this study. We also thank Dr. John Mount for assistance with Mathematica.

REFERENCES

- Mann, K. G., Jenny, R. J., and Krishnaswamy, S. (1988) *Annu. Rev. Biochem.* 57, 915–956.
- Müller-Eberhard, H. J. (1988) *Annu. Rev. Biochem.* 57, 321–347.
- Seidah, N. G., and Chrétien, M. (1997) *Curr. Opin. Biotechnol.* 8, 602–607.
- Steiner, D. F., Smeeckens, S. P., Ohagi, S., and Chan, S. J. (1992) *J. Biol. Chem.* 267, 23435–23438.
- Döring, G. (1994) *Am. J. Respir. Crit. Care Med.* 150, S114–S117.
- Werb, Z. (1997) *Cell* 91, 439–442.
- Schmitt, M., Jänicke, F., and Graeff, H. (1992) *Fibrinolysis* 6, 3–26.
- Katz, B. A., Clark, J. M., Finer-Moore, J. S., Jenkins, T. E., Johnson, C. R., Luong, C., Moore, W. R., and Stroud, R. M. (1998) *Nature* 391, 608–612.
- Schwartz, L. B. (1994) *Methods Enzymol.* 244, 88–100.
- Schwartz, L. B. (1990) *J. Allergy Clin. Immunol.* 86, 94–98.
- Sekizawa, K., Caughey, G. H., Lazaris, S. C., Gold, W. M., and Nadel, J. A. (1989) *J. Clin. Invest.* 83, 175–179.
- Clark, J. M., Abraham, W. M., Fishman, C. E., Forteza, R., Ahmed, A., Cortes, A., Warne, R. L., Moore, W. R., and Tanaka, R. D. (1995) *Am. J. Respir. Crit. Care Med.* 152, 2076–2083.
- Butterfield, J. H., Weiler, D. A., Hunt, L. W., Wynn, S. R., and Roche, P. C. (1990) *J. Leukocyte Biol.* 47, 409–419.
- Church, T. J., Cutshall, N. S., Gangloff, A. R., Jenkins, T. E., Linsell, M. S., Litvak, J., Rice, K. D., and Spencer, J. R. (1998) PCT Int. Appl. WO 9845275.
- Tuppy, H., Weisbauer, U., and Wintersberger, E. (1962) *Hoppe-Seyler's Z. Physiol. Chem.* 329, 278–288.
- Kuzmic, P. (1996) *Anal. Biochem.* 237, 260–273.
- Kurganov, B. I., Sugrobova, N. P., and Yakovlev, V. A. (1972) *FEBS Lett.* 19, 308–310.
- Morrison, J. F. (1969) *Biochim. Biophys. Acta* 185, 269–286.
- Marquardt, D. W. (1963) *J. Soc. Ind. Appl. Math.* 11, 431–441.
- Connors, K. A. (1987) in *Binding Constants: The Measurement of Molecular Complex Stability*, pp 141–187, John Wiley and Sons, New York.
- Cleland, W. W. (1979) *Methods Enzymol.* 63, 103–138.
- Yonetani, T., and Theorell, H. (1964) *Arch. Biochem. Biophys.* 106, 243–251.
- Morrison, J. F., and Walsh, C. T. (1988) *Adv. Enzymol.* 61, 201–301.
- Masuoka, J., Hegenauer, J., Van Dyke, B. R., and Saltman, P. (1993) *J. Biol. Chem.* 268, 21533–21537.
- Berthon, G., Matuchansky, C., and May, P. (1980) *J. Inorg. Biochem.* 13, 63–73.
- Tidwell, R. R., Gratz, J. D., Dann, O., Volz, G., Zeh, D., and Loewe, H. (1978) *J. Med. Chem.* 21, 613–623.
- Christianson, D. W. (1991) *Adv. Protein Chem.* 42, 281–355.
- Smith, R. M., and Martell, A. E. (1975) in *Critical Stability Constants, Vol. 2: Amines*, pp 144–255, Plenum Press, New York.
- Irving, H., and Williams, R. J. P. (1948) *Nature* 162, 746–749.
- Yonetani, T. (1982) *Methods Enzymol.* 87, 500–509.
- Martinez-Irujo, J. J., Villahermosa, M. L., Mercapide, J., Cabodevilla, J. F., and Santiago, E. (1998) *Biochem. J.* 329, 689–698.
- Morrison, J. F., and Stone, S. R. (1985) *Comments Mol. Cell. Biophys.* 2, 347–368.
- Cha, S. (1975) *Biochem. Pharmacol.* 24, 2177–2185.
- Schloss, J. V. (1988) *Acc. Chem. Res.* 21, 348–353.
- Vallee, B. L. (1983) in *Zinc Enzymes* (Spiro, T. G., Ed.) pp 1–24, John Wiley and Sons, New York.
- Masuoka, J., and Saltman, P. (1994) *J. Biol. Chem.* 269, 25557–25561.
- Peters, T., Jr. (1985) *Adv. Protein Chem.* 37, 161–245.
- Vallee, B. L., and Auld, D. S. (1990) *Biochemistry* 29, 5647–5659.
- Berg, J. M., and Shi, Y. (1996) *Science* 271, 1081–1085.
- O'Halloran, T. V. (1993) *Science* 261, 715–725.
- Lipscomb, W. N., and Sträter, N. (1996) *Chem. Rev.* 96, 2375–2433.
- Somers, W., Ultsch, M., De Vos, A. M., and Kossiakoff, A. A. (1994) *Nature* 372, 478–481.
- Bernardo, M. M., Day, D. E., Olson, S. T., and Shore, J. D. (1993) *J. Biol. Chem.* 268, 12468–12476.
- Higaki, J. N., Haymore, B. L., Chen, S., Fletterick, R. J., and Craik, C. S. (1990) *Biochemistry* 29, 8582–8586.
- Magneson, G. R., Puvathingal, J. M., and Ray, W. J., Jr. (1987) *J. Biol. Chem.* 262, 11140–11148.
- Schroeder, H. A., and Nason, A. P. (1971) *Clin. Chem.* 17, 461–473.
- Giroux, E. L., Durieux, M., and Schechter, P. J. (1976) *Bioinorg. Chem.* 5, 211–218.
- Parisi, A. F., and Vallee, B. L. (1970) *Biochemistry* 9, 2421–2426.
- Harris, W. R., and Keen, C. (1989) *J. Nutr.* 119, 1677–1682.

BI992182J